metals

MDPI

Article

Investigation of the Possibility of Tailoring the Chemical Com-Position of the NiTi Alloy by Selective Laser Melting

Evgenii Borisov [1,*], Kirill Starikov [1], Anatoly Popovich [1] and Tatiana Tihonovskaya [2]

[1] Peter the Great St. Petersburg Polytechnic University (SPbPU), Polytechnicheskaya 29, 195251 St. Petersburg, Russia; kirill.starikov@gmail.com (K.S.); director@immet.spbstu.ru (A.P.)
[2] Private Institution for Ensuring the Scientific Development of the Nuclear Industry "Science and Innovations", State Corporation "Rosatom", 115035 Moscow, Russia; TaATikhonovskaya@rosatom.ru
* Correspondence: evgenii.borisov@icloud.com

Abstract: In this work a study of the selective laser melting process of two NiTi alloys of equiatomic, and rich Ni composition were conducted. A study of the influence of the technological parameters on the alloy density was carried out. Values of technological parameters were obtained to ensure production of samples with the lowest number of defects. When using process parameters with the same energy density but different values of the constituent technological parameters, the amount of nickel carried away by evaporation changed insignificantly. An increase in the energy density led to an increase in the amount of nickel carried away, causing final samples with lower Ni content. When using multiple laser processing in the low-energy parameter set, it was possible to achieve a decrease in the nickel content in the alloy, similar to that with single high-energy processing. DSC studies showed a significant increase in transformation temperatures upon repeated laser processing due to the higher evaporation of nickel. The use of double laser treatment gave a decrease in the final density of the sample compared to a single treatment, but its value is still higher than when using a single treatment with a higher energy density.

Keywords: powder metallurgy; additive manufacturing; nitinol; selective laser melting; laser

Citation: Borisov, E.; Starikov, K.; Popovich, A.; Tihonovskaya, T. Investigation of the Possibility of Tailoring the Chemical Com-Position of the NiTi Alloy by Selective Laser Melting. *Metals* **2021**, *11*, 1470. https://doi.org/10.3390/met11091470

Academic Editor: Christian Mittelstedt

Received: 29 July 2021
Accepted: 13 September 2021
Published: 16 September 2021

1. Introduction

The development of modern industry, the creation of digital infrastructure and the widespread introduction of digital devices have given rise to the development of "smart" devices and technologies. In new products and assemblies, almost every material used is tailored with task-specific properties. As a result of this, functional materials have become widespread, exhibiting specific characteristics which depend on the properties required from them. Composite and gradient materials, in which the characteristics are not uniformly distributed through the volume, can provide the necessary properties in the best zones for this.

One of the groups of functional materials is shape memory alloys (SMA), which open up new possibilities in modern science and technology. With their appearance, it became possible to set in motion mechanisms and structural elements without the use of specialized actuators, motors and other devices [1]. Nitinol (NiTi) is an SMA of titanium with nickel. This alloy was first patented in 1965 by W. Buger and F. Wang of the United States Naval Laboratory [2]. At the end of the 1960s, the first practical application of this NiTi alloy was in aircraft construction to form a coupling in the hydraulic system of the F-14 fighter jets [3]. Further study and research of NiTi alloys made it possible to partially expand their applicability, based on their ability to exhibit the shape memory effect, which is activated at certain temperatures and develops a certain force.

Depending on the nickel content, nitinol may show either shape memory effect (SME) and super elasticity (SE) [4]. Equiatomic nitinol (50 at.% Ni) exhibits SME at room temperature. In the initial state (at a low temperature and in a relaxed state), nitinol consists

of twinned martensite. When a load is applied, a reorientation called detwinning begins. During unloading, this structure is retained, as well as the resulting deformation. When the material is heated above the temperature of the onset of austenite transformation (As), the transformation of martensite into austenite begins, which ends at a austenite finish temperature (Af). This restores the original shape of the product [5]. At temperatures above Af, the effect of superelasticity appears. With an increase in the nickel content, the values of the transformation temperatures decrease, and at some values of the content, the alloy can exhibit the effect of super elasticity at room temperature [4]. Currently, alloys of the NiTi system with SME or SE are used in the aerospace industry [6], medicine [7], there are various developments and applications in the automotive industry and other devices [8,9]. NiTi alloys can play various roles including temperature sensors, thermo-force actuators, thermomechanical connectors, various implants with SME, stents and tightening bone fixators [4,5,10].

Despite a certain share of NiTi system alloys in industry, their use is still extremely limited. This is primarily due to the high cost and complexity of production, and the serious and complex influence of the processing parameters on the final alloy properties (including how it performs). These factors create certain difficulties in obtaining NiTi products in complex shapes when classical processing methods are used [11,12].

The emergence and development of additive manufacturing technologies has changed the approach in manufacturing NiTi system alloys and the products made from them [13]. Additive technologies have made it possible to manufacture products of complex shape without additional machining from powders of various alloys. Concerning the manufacture of products from NiTi system powders, the term 4D printing is used [14]. According to [15], the term 4D printing relates to the technique of using additive manufacturing on stimulus-responsive active materials which results in a physical or chemical change in their composition with time [16–20].

For an actuator based on the SME, its behavior greatly depends on the geometric shape of the main element, and its chemical composition. There are several works [21–29], which noted a change in the chemical composition of the NiTi alloys during laser processing. This was caused by a decrease in the concentration of nickel due to evaporation. Under present methods, routes to carefully control the chemical composition of nitinol alloy are yet to be found. There are several studies devoted to the study of the influence of the SLM process parameters on the composition of elements in the NiTi alloy.

There have been studies testing the influence of various parameter sets with different single parameters but same volume energy density [23,28,29]. In paper [23] it was shown that the Ni content in all of the NiTi fabricated samples was 55.3–55.4 wt%, which showed no obvious difference when compared with the starting NiTi powders (55.4 wt%). At the same time, in [28,29] a significant difference was found between the chemical composition of the samples with same energy density.

In [24] investigations were carried out of the dependence of the composition and properties of two NiTi alloys depending on the energy density of the parameter set used. It was found that the temperatures of phase transformations increase almost monotonically with the volumetric energy density used for printing due to the Ni evaporation during the melting process. Consequently, it is shown that it is possible to fine-tune the chemical composition and functional properties of NiTi alloys with a high nickel content by varying the processing parameters, which was implemented in [25]. However, with an increase in the energy density to a certain value, the formation of keyhole porosity begins, which reduces the total density of the samples and increases the number of defects [30]. This limits the ability to control the composition of the samples.

Thus, the purpose of this work was to study the effect of selective laser melting (SLM) process parameters on changes in the Ni content and density of the NiTi alloys with different initial chemical compositions. Also, determination of the possibility to effectively control the chemical composition of samples without using high-energy parameter sets, which lead to the formation of defects in the samples.

2. Materials and Methods

Commercial powders of NiTi alloys were gas atomized and supplied by CNPC Powder (CNPC Powder, Shanghai, China) and were used as the initial material. For this study, a sample with a near-equiatomic composition, and a sample with a high nickel content were selected, designated as NiTi 50.0 and NiTi 50.7, respectively (composition of initial powders 50.3% of Ni for NiTi 50.0 and 51.02 for NiTi 50.7). The particle size distribution was measured with a Fritsch Analysette 22 Laser Particle Sizer (Fritsch GmbH, Idar-Oberstein, Germany). The particle sizes were d10 = 22.4 μm, d50 = 39.4 μm, d90 = 66.3 μm for 50.0 Ni, and d10 = 26.7 μm, d50 = 49.6 μm, d90 = 84.6 μm for 50.7 Ni. Samples were prepared using an Aconity3D MIDI (Aconity3D GmbH, Herzogenrath, Germany) selective laser melting machine. The machine is equipped with a laser with a power of one kilowatt. To study the chemical composition of powders and compact samples, a TESCAN Mira 3 LMU scanning electron microscope (TESCAN, Brno, Czech Republic) with an EDX X-max 80 energy dispersive spectrometer manufactured by Oxford Instruments are used. Measurements were carried out over 10 areas of the sample microsection, after which the average value and standard deviation of the composition were calculated. The density of the samples was carried out using the Archimedes method. Two cubic samples were made for each parameter set. Each sample was tested three times, and the average of all measurements was taken as the density value of the sample. Sample microstructure was studied on pre-polished and etched microsections of the specimens using a Leica DMI 5000 optical microscope (Leica Microsystems, Wetzlar, Germany). Differential scanning calorimetry (DSC) measurements were used to study the transformation temperatures.

To study the process of selective laser melting and the dependence of the density and chemical composition of the manufactured samples on the values of process parameters, the values presented in Table 1 were used. A range of laser power values from 175 to 225 watts with a step of 25 watts and a range scanning speeds from 800 to 1050 mm/s with a step of 125 mm/s were selected. Laser beam diameter for all parameter sets was ~80 μm. When the parameter sets were formed, the power and speed of laser radiation were simultaneously increased so as to keep the volumetric energy density constant (60 J/mm^3). In addition to the three-parameter sets, there were two parameter sets with constant laser power were used, differing only in the speed of laser radiation. For them, the average value (200 watts) was chosen as the power, and the extreme values (for the A4 mode—1050 mm/s, for the A5 mode—800 mm/s) were chosen as the laser scanning speed. The volumetric energy density at the selected parameters of power and scanning speed, and the distance between the laser hatches equal to 0.120 mm, is in the range of ~53–69 J/mm^3.

Table 1. Parameter sets of sample preparation by selective laser melting.

Parameter Set	Power, W	Velocity, mm/s	Hatch Distance, mm	Layer Thickness, mm	Energy Density, J/mm^3
A1	175	800	0.12	0.03	60
A2	200	925	0.12	0.03	60
A3	225	1050	0.12	0.03	60
A4	200	1050	0.12	0.03	53
A5	200	800	0.12	0.03	70

Based on these parameter sets, further sets were selected, to investigate their influence on the chemical composition of samples. The selected parameter sets are shown in Table 2.

Parameter sets were selected in such a way as to conduct a study of the bearing of various parameters on the SLM process and to identify those that had the greatest impact. In parameter sets 1, 2, 5, and 6 the scanning speed of the laser beam was changed. In parameter sets 1 and 3, the laser radiation power was changed. Parameter sets 1 and 4 differ from each other in that they use different distances between the individual hatches.

Table 2. Selective laser melting parameters for the preparation of compact samples.

Parameter Set	Power, W	Velocity, mm/s	Hatch Distance, mm	Layer Thickness, mm	VED, J/mm^3
1	250	800	0.12	0.03	86.8
2	250	400	0.12	0.03	173.6
3	350	800	0.12	0.03	121.5
4	250	800	0.08	0.03	130.2
5	250	1000	0.12	0.03	69.4
6	250	1200	0.12	0.03	55.0

To investigate the possibility of changing the energy density for each layer, without using high-energy process parameters, a study of multiple laser processing was carried out. The essence of this method was that after the main laser treatment was carried out, reprocessing was started according to the same parameters and according to the same strategy. Thus, for the first time, the main melting of the powder material and the formation of a continuous layer occurred. During the second time, the laser treatment went along the previously-formed layer with no additional powder material applied. The process parameters used to study the effect of laser treatment are shown in Table 3. Parameter set 6 with the lowest value of VED and parameter set 4 with the highest non-destructive VED value were selected. The VED value of parameter set 6 allows 3 repeated scans, but the VED value of parameter set 4 is too high and overheating of the sample surface occurs during triple scanning.

Table 3. Parameter sets used for double and triple laser processing.

Parameter Set	Power, W	Velocity, mm/s	Hatch Distance, mm	Layer Thickness, mm	Energy Density, J/mm^3	Number of Treatments
4_2	250	800	0.08	0.03	130.2	2
6_2	250	1200	0.12	0.03	55.0	2
6_3	250	1200	0.12	0.03	55.0	3

Parameter set 4_2 is a modification of 4, but with double laser treatment. Similarly, parameter set 6_2 is double processing of 6, and 6_3 is a parameter set 6 with triple processing.

3. Results and Discussion

3.1. Selective Laser Melting

Applying the high-volume energy density resulted in a distorted surface (Figure 1), which may occur due to a large depth of penetration and the formation of a large melt pool [31]. A large volume in the melt pool leads to an increase in the number of powder particles wetted and drawn into the melt. This phenomenon leads to a distortion of the geometry of the surface layer.

A strong distortion of the surface layer prevents the movement of the recoater and does not allow the process of selective laser melting to continue. To solve this problem, we used repeated scanning with a lower volume energy density parameter. During repeated scanning there is no distortion of the sample surface layer. This effect occurs due to the reduction of the melt pool.

3.2. Density Measurement

Results of density measurements given in Table 4. Density values are close, but the highest value in both materials (NiTi 50.0 and NiTi 50.7) belong to parameter set A4, which has the lowest value of VED. With an increase in the energy density, the formation of keyhole defects is possible, which reduces the overall level of the specimens [30]. The average density values of compact sample groups from NiTi 50.7 alloy are ~0.01 g/cm^3 higher than the similar density values of compact samples from the NiTi 50.0 alloy, which is explained by the high percentage of Ni by 0.7% and which has a higher density than

titanium. In addition, differences in density can be caused by differences in the original particle size distribution of the powders (NiTi 50.7 powder is coarser). The obtained density values will be used in the future to compare the effect of high-energy modes, as well as double laser treatment on the density of samples.

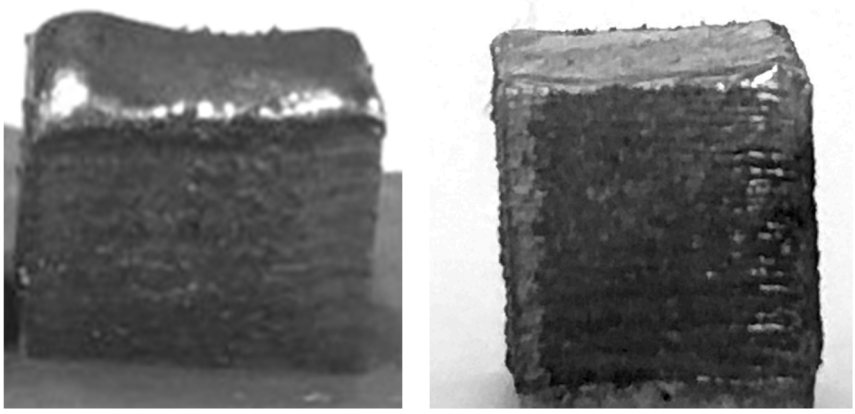

(**a**) (**b**)

Figure 1. A sample prepared by selective laser melting from NiTi 50.7 alloy powder. (**a**) with VED = 173.6 J/mm^3, parameter set 2 (Table 2); (**b**) with VED = 130.2 (×2) J/mm^3, parameter set 4_2 (Table 3).

Table 4. Density of samples made by selective laser melting.

Parameter Set	Density, g/cm^3	
	NiTi 50.0	NiTi 50.7
A1	6.45	6.46
A2	6.45	6.45
A3	6.45	6.46
A4	6.46	6.47
A5	6.45	6.46

3.3. Chemical Composition

The parameters of the SLM process can affect not only the structure of NiTi SMA but also their chemical composition. When studying the influence of the selective laser melting process parameters on the characteristics of the resulting material, the energy density parameter is used, which is calculated by the formula:

$$E_v = P/(\nu * h * t) \quad (1)$$

where E_v is the volumetric energy density, [J/mm^3], P is the power of the laser radiation, [W], ν is the speed of the laser beam, [mm/s], h is the distance between the individual hatches of the laser beam, [mm], t-layer thickness, [mm].

Thus, it is possible to influence the energy density using differing parameters, the influence of which may vary at similar values of the energy density. Therefore, for example, increasing the power of the laser radiation increases the amount of energy imparted to the surface, which is currently exposed to the laser radiation. An increase in the speed of movement of the laser source reduced the duration of exposure of the laser source to the treated surface. This contributed to a lower energy input into the part, however, it led to higher temperature gradients. In turn, a change in the distance between individual laser hatches led to a change in the distance between the tracks of the melt baths, thereby changing the number of laser hatches in each layer, the duration of laser irradiation of the entire part, while not affecting the melt bath directly.

Table 5 shows the results of the samples chemical composition measurements according to parameter set A1–A3 (with an energy density of 60 J/mm^3).

Table 5. The results of studying the chemical composition of powder and samples after the SLM process.

Sample	Parameter Set	Ni, at.%	Ti, at.%
Powder NiTi 50	-	50,3	49.7
Powder NiTi 50.7	-	51.02	48.98
SLM NiTi 50.0	A1	50.23	49.77
	A2	50.22	49.78
	A3	50.20	49.80
SLM NiTi 50.7	A1	50.89	49.11
	A2	50.87	49.13
	A3	50.88	49.12

As can be seen, although the parameters of the SLM process changed significantly, the chemical composition of the alloys remained near constant, which is consistent with [23]. The level of nickel evaporation from both powders was in the range of 0.07–0.15%. In all the samples obtained, the nickel content was less than the initial material. This is primarily due to the evaporation of nickel during processing. Since nickel has a lower boiling point than titanium, its partial evaporation occurred during the scanning and remelting of material layers in the SLM process.

Table 6 shows the results of studying the chemical composition of the alloy samples made with different energy density (parameter sets from Table 2). The compositions of the samples obtained under different parameter sets differ. For parameter set number 6 with a bulk energy density of 55.5 J/mm^3 (the lowest among all parameter sets), the level of nickel evaporation was no more than 0.1 at.%. At the same time, for the parameter set No. 2 with a volumetric energy density of 173.6 J/mm^3, the level of evaporation was more than 1 at.%.

Table 6. The results of studying the chemical composition of samples of the alloy NiTi 50 and NiTi 50.7, obtained by the SLM method in different parameter sets.

Sample	Parameter Set	Ni, at.%	Ti, at.%
SLM NiTi 50.0	1	50.03	49.97
	2	49.28	50.72
	3	49.96	50.04
	4	49.69	50.31
	5	50.1	49.90
	6	50.21	49.79
SLM NiTi 50.7	1	50.88	49.12
	2	50.44	49.56
	3	50.88	49.12
	4	50.71	49.29
	5	50.88	49.12
	6	50.84	49.16

For an alloy with a nickel content of 50.7% in the energy density range from 55 to 100 J/mm^3, no significant dependence of the nickel content on the energy density was observed. The samples obtained by parameter sets 1, 3, and 5 (energy densities 86.8 J/mm^3, 121.5 J/mm^3, and 69.4 J/mm^3 respectively), had a nickel content of 50.88 at.%, which is more than that of the sample obtained by parameter set No. 6 (50.84 at.% Ni) at an energy density of 55.5 J/mm^3.

For greater clarity, Figure 2 shows the dependence of the nickel content in the alloy on the bulk energy density of the SLM process. With an increase in this bulk energy

density, the nickel content in the alloy decreased owing to evaporation under high-energy conditions. Similar dependencies were observed for the NiTi 50.0 alloy.

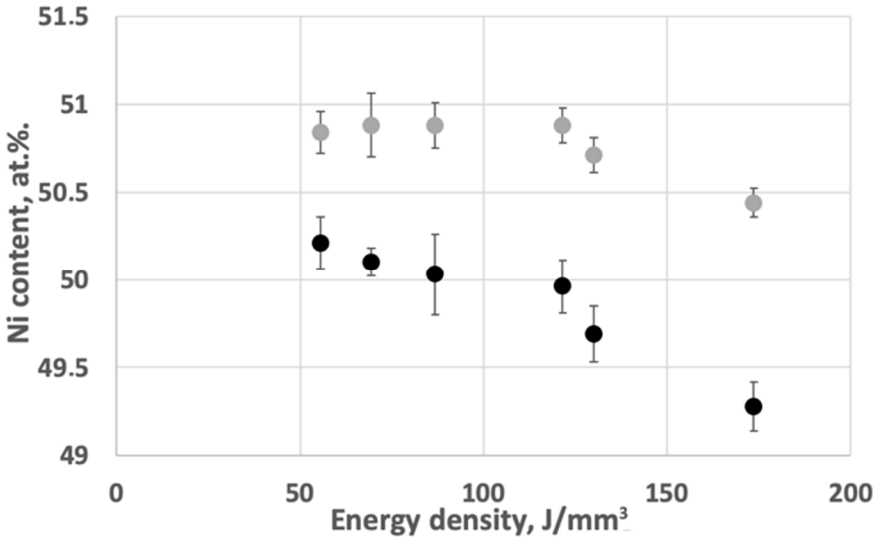

Figure 2. Dependence of the Ni content in compact samples on the bulk energy density during the SLM process. Black—NiTi 50.0, gray—NiTi 50.7.

Table 7 shows the results of the chemical composition of studied alloy samples manufactured with two and three repeated treatments (parameter sets from Table 3). An increase in the number of re-treatments led to an increase in the level of evaporation of nickel. With two repeated treatments nickel level decreased from 50.21 at.% for the parameter set 6 to 49.94 at.% for 6_2. Using three treatments reduced the nickel level further. Such changes are explained by the fact that during repeated treatments, the previously formed layer is re-melted. This leads to additional evaporation of nickel from the alloy.

Table 7. The results of the study of the chemical composition of the alloy samples NiTi 50.0 and NiTi 50.7, obtained by the SLM method in a different modes.

Sample	Parameter Set	Ni, at.%	Ti, at.%
SLM NiTi 50.0	4_2	49.82	50.18
	6_2	49.94	50.06
	6_3	49.6	50.4
SLM NiTi 50.7	4_2	50.54	49.46
	6_2	50.40	49.60
	6_3	50.43	49.57

As can be seen from Figure 3, an increase in the number of treatments leads to a decrease in the nickel content, which falls from 50.2 at.% for a single treatment to 49.6 at.% for three successive treatments, with the same manufacturing parameters used for each laser treatment. For the NiTi 50.7 alloy, a similar dependence was observed.

Thus, double treatment of NiTi 50.0 alloy according to parameter set number 6 (with an energy density of 55.5 J/mm^3) results in similar chemical composition with a single treatment with parameter set number 3 (with an energy density of 121.5 J/mm^3). A similar double treatment of the NiTi 50.7 alloy results in chemical composition, close to a single treatment with parameter set number 2 (with an energy density of 173.6 J/mm^3).

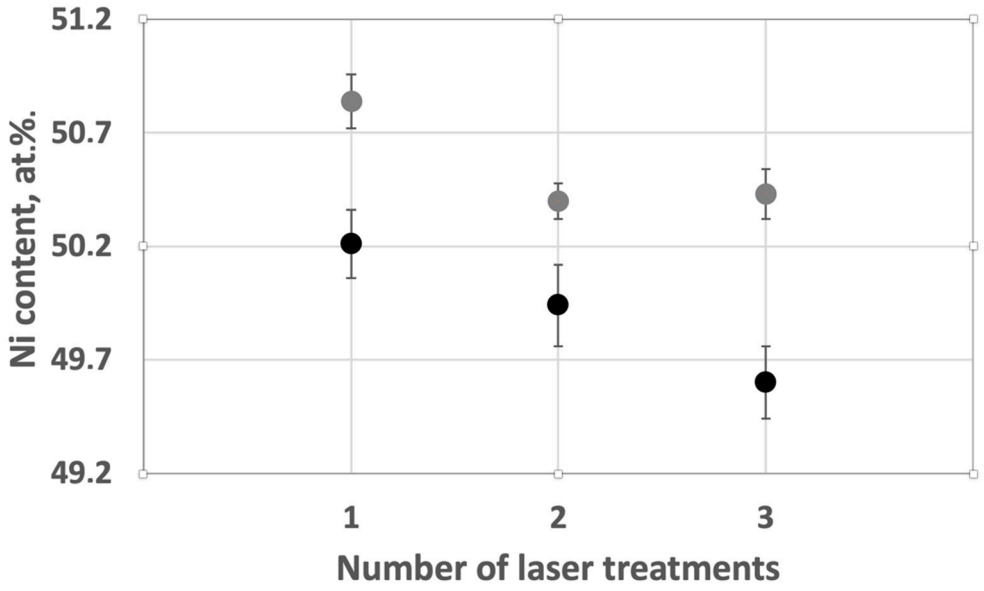

Figure 3. Dependence of the Ni content in compact samples on the number of laser treatments. Black dots—50.0, gray dots—50.7.

3.4. DSC Measurements

To study the effect of different processing methods on the characteristic temperatures of phase transformation, the DSC curves of samples made from the NiTi 50.7 alloy powder according to parameter sets 2, 4, 4_2 (Figure 4) were taken. The energy densities of the parameter sets were 173.6, 130.2, and 2 × 130.2 J/mm^3, respectively. Table 8 summarizes the results of the DSC study of the samples.

A single treatment according to parameter set 2 gives higher temperatures of phase transformation than for parameter set 4 with a single treatment, and lower than in parameter set 4_2 with double treatment. A change in the energy density by 43 J/mm^3 for single treatment gave an increase in the temperature of the beginning of the martensitic transformation of the NiTi 50.7 alloy by 34 degrees due to the evaporation of nickel, which is consistent with [24]. The decrease in the energy density for a single laser treatment led to some broadening of the peaks. The width of the peaks is wider at lower energy densities, which was also previously obtained in [26,27,30]. When using double laser processing, the width of the martensitic transformation interval becomes even wider, apparently due to uneven evaporation of nickel. Annealing can lead to a narrowing of the peaks with a simultaneous slight decrease in the transformation temperatures [30], however, this requires further study.

Table 8. Martensitic phase transformation temperatures of the NiTi 50,7 specimens.

Parameter Set	VED, J/mm^3	M_s (°C)	M_f (°C)	A_s (°C)	A_f (°C)	A_f-A_s (°C)	Density, g/cm^3
2	173.6	6	−23	9	30	21	6.32
4	130.2	−28	−66	−27	−4	23	6.44
4_2	130.2 (×2)	24	−13	18	54	36	6.38

When using a regime with a higher energy density, the density of the samples decreases, as it was shown earlier in this work and in, for instance, in [30]. When using double laser processing, the final density of the sample decreased compared to a single processing, but its value is still higher than when using a single processing with a higher energy density.

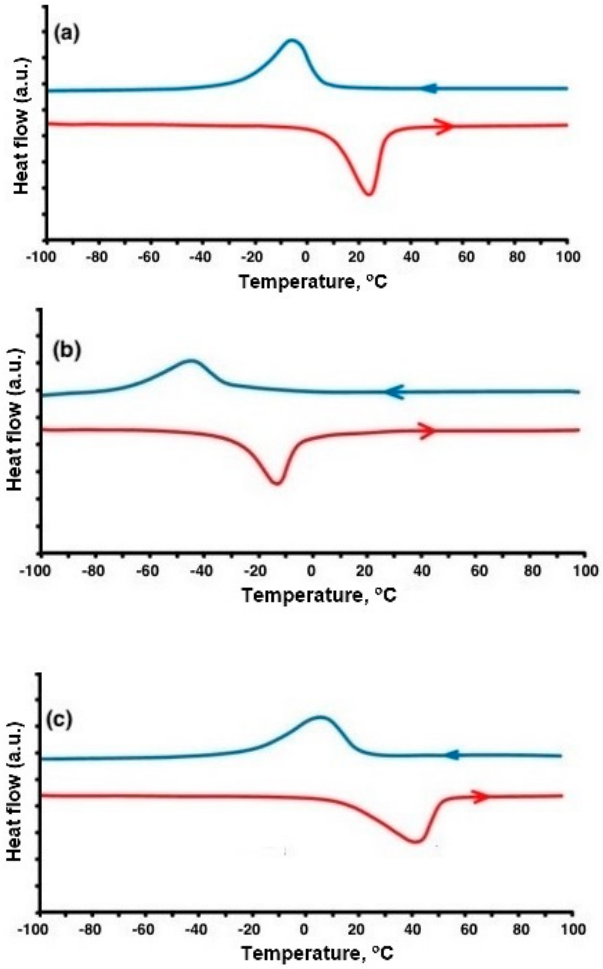

Figure 4. DSC curves for samples made from NiTi 50.7 powder with parameter sets 2 with VED = 173.6 J/mm^3 (**a**), parameter set 4 with VED = 130.2 J/mm^3 (**b**), parameter set 4_2 with VED = 130.2 × 2 J/mm^3 (**c**) according to Tables 2 and 3.

Due to the lower stability of the SLM process when using high-energy parameter sets to control the nickel content in the alloy [31], the approach of using multiple processing in fewer energy sets can be used. Thus, it is possible to adjust the nickel content to obtain the required transformation temperatures.

Thus, using parameter sets with higher VED values, it is possible to control the microstructure and phase composition of materials. This effect is set locally to create products with variable DSC curves (Figure 4). However, the above image of the sample layer surface (Figure 1a) excludes this possibility. The principle of repeated scanning considered in the article solves the problem of damage to the layer surface (Figure 1b) and can be used for a functional gradient over the volume of the product.

4. Conclusions

A study was carried out upon the selective laser melting process on NiTi alloys with different proportions of nickel. The use of parameter sets with the same energy density but with different values of individual parameters did not lead to significant differences in the final chemical composition of the samples. When using sets of parameters with different energy densities in both alloys, a decrease in the nickel content is observed with an increase in the energy density. With an increase in the energy density by a factor of 3.5, the nickel content in the alloy of the Ti-50% Ni system decreased from 50.21% to 49.28%.

The dependence of the nickel content in the alloy on the energy density and the number of laser treatments has been established. It was found that when using multiple

laser processing in the low-energy parameter set, it was possible to achieve a decrease in the nickel content in the alloy, similar to that with single high-energy processing with the formation of a higher density value. DSC studies showed a significant increase in transformation temperatures upon repeated laser processing due to the higher evaporation of nickel.

Author Contributions: T.T., A.P.: conceptualization, formal analysis; K.S., E.B. and A.P.: investigation; K.S. and E.B.: methodology; A.P.: supervision; T.T.: validation; K.S., E.B. and A.P.: visualization; K.S. and E.B.: writing—original draft; A.P.: writing—review & editing. All authors have read and agreed to the published version of the manuscript.

Funding: This study was carried out under the State Contract dated 04.06.2020 №Н.4ш.241.09.20.1081 (ИГК 17706413348200001110).

Institutional Review Board Statement: Not applicable.

Informed Consent Statement: Not applicable.

Data Availability Statement: The data presented in this study are available on request from the corresponding author.

Conflicts of Interest: The authors declare no conflict of interest.

References

1. Russell, R.A.; Gorbet, R.B. Improving the response of SMA actuators. In Proceedings of the 1995 IEEE International Conference on Robotics and Automation, Nagoya, Japan, 21–27 May 1995; Volume 3, pp. 2299–2304.
2. Buehler, W.J.; Wiley, R.C. Nickel-Base Alloys. U.S. Patent 3,174,851, 23 March 1965.
3. Mantovani, D. Shape memory alloys: Properties and biomedical applications. *JOM* **2000**, *52*, 36–44. [CrossRef]
4. Jani, J.M.; Leary, M.; Subic, A.; Gibson, M.A. A review of shape memory alloy research, applications and opportunities. *Mater. Des.* **2014**, *56*, 1078–1113. [CrossRef]
5. Behera, A.; Rajak, D.K.; Kolahchi, R.; Scutaru, M.-L.; Pruncu, C.I. Current global scenario of Sputter deposited NiTi smart systems. *J. Mater. Res. Technol.* **2020**, *9*, 14582–14598. [CrossRef]
6. Quan, D.; Hai, X. Shape Memory Alloy in Various Aviation Field. *Procedia Eng.* **2015**, *99*, 1241–1246. [CrossRef]
7. Guo, S.; Fukuda, T. SMA actuator-based novel type of micropump for biomedical application. In Proceedings of the IEEE International Conference on Robotics and Automation, New Orleans, LA, USA, 26 April–1 May 2004; Volume 2, pp. 1616–1621.
8. Williams, E.; Elahinia, M.H. An automotive SMA mirror actuator: Modeling, design, and experimental evaluation. *J. Intell. Mater. Syst. Struct.* **2008**, *19*, 1425–1434. [CrossRef]
9. Miková, L.; Medvecká-Beňová, S.; Kelemen, M.; Trebuňa, F.; Virgala, I. Application of shape memory alloy (SMA) as actuator. *Metalurgija* **2015**, *54*, 169–172.
10. Nematollahi, M.; Baghbaderani, K.S.; Amerinatanzi, A.; Zamanian, H.; Elahinia, M. Application of NiTi in Assistive and Rehabilitation Devices: A Review. *Bioengineering* **2019**, *6*, 37. [CrossRef] [PubMed]
11. Otsuka, K.; Wayman, C.M. (Eds.) *Shape Memory Materials*; Cambridge University Press: Cambridge, UK, 1999.
12. Van Humbeeck, J. Non-medical applications of shape memory alloys. *Mater. Sci. Eng. A* **1999**, *273–275*, 134–148. [CrossRef]
13. Kim, A.; Makhmutov, T.; Razumov, N.; Silin, A.; Popovich, A.; Zhu, J.-N.; Popovich, V. Synthesis of NiTi alloy powders for powder-based additive manufacturing. *Mater. Today Proc.* **2020**, *30*, 679–682. [CrossRef]
14. Khoo, Z.X.; Teoh, J.E.M.; Liu, Y.; Chua, C.K.; Yang, S.; An, J.; Leong, K.F.; Yeong, W.Y. 3D printing of smart materials: A review on recent progresses in 4D printing. *Virtual Phys. Prototyp.* **2015**, *10*, 103–122. [CrossRef]
15. Pei, E. 4D Printing: Dawn of an emerging technology cycle. *Assem. Autom.* **2014**, *34*, 310–314. [CrossRef]
16. Ntouanoglou, K.; Stavropoulos, P.; Mourtzis, D. 4D Printing Prospects for the Aerospace Industry: A critical review. *Procedia Manuf.* **2018**, *18*, 120–129. [CrossRef]
17. Polozov, I.; Sufiiarov, V.; Popovich, A.; Masaylo, D.; Grigoriev, A. Synthesis of Ti-5Al, Ti-6Al-7Nb, and Ti-22Al-25Nb alloys from elemental powders using powder-bed fusion additive manufacturing. *J. Alloy. Compd.* **2018**, *763*, 436–445. [CrossRef]
18. Goncharov, I.; Razumov, N.; Silin, A.; Ozerskoi, N.; Shamshurin, A.; Kim, A.; Wang, Q.; Popovich, A. Synthesis of Nb-based powder alloy by mechanical alloying and plasma spheroidization processes for additive manufacturing. *Mater. Lett.* **2019**, *245*, 188–191. [CrossRef]
19. Razumov, N.G.; Popovich, A.A.; Grigor'Ev, A.V.; Silin, A.O.; Goncharov, I.S. Morphology of high-strength heat-resistant steel powder for machines for additive production from shavings. *Met. Sci. Heat Treat.* **2019**, *60*, 710–714. [CrossRef]
20. Farber, E.; Zhu, J.-N.; Popovich, A.; Popovich, V. A review of NiTi shape memory alloy as a smart material produced by additive manufacturing. *Mater. Today Proc.* **2020**, *30*, 761–767. [CrossRef]
21. Dadbakhsh, S.; Speirs, M.; Kruth, J.-P.; Schrooten, J.; Luyten, J.; Van Humbeeck, J. Effect of SLM Parameters on Transformation Temperatures of Shape Memory Nickel Titanium Parts. *Adv. Eng. Mater.* **2014**, *16*, 1140–1146. [CrossRef]

22. Speirs, M.; Wang, X.; Van Baelen, S.; Ahadi, A.; Dadbakhsh, S.; Kruth, J.-P.; Van Humbeeck, J. On the Transformation Behavior of NiTi Shape-Memory Alloy Produced by SLM. *Shape Mem. Superelasticity* **2016**, *2*, 310–316. [CrossRef]
23. Chen, W.; Yang, Q.; Huang, S.; Huang, S.; Kruzic, J.J.; Li, X. Laser power modulated microstructure evolution, phase transformation and mechanical properties in NiTi fabricated by laser powder bed fusion. *J. Alloy. Compd.* **2020**, *861*, 157959. [CrossRef]
24. Xue, L.; Atli, K.; Picak, S.; Zhang, C.; Zhang, B.; Elwany, A.; Arroyave, R.; Karaman, I. Controlling martensitic transformation characteristics in defect-free NiTi shape memory alloys fabricated using laser powder bed fusion and a process optimization framework. *Acta Mater.* **2021**, *215*, 117017. [CrossRef]
25. Nematollahi, M.; Safaei, K.; Bayati, P.; Elahinia, M. Functionally graded NiTi shape memory alloy: Selective laser melting fabrication and multi-scale characterization. *Mater. Lett.* **2021**, *292*, 129648. [CrossRef]
26. Lu, H.; Yang, C.; Luo, X.; Ma, H.; Song, B.; Li, Y.; Zhang, L. Ultrahigh-performance TiNi shape memory alloy by 4D printing. *Mater. Sci. Eng. A* **2019**, *763*, 138166. [CrossRef]
27. Yang, Y.; Zhan, J.; Sun, Z.; Wang, H.; Lin, J.; Liu, Y.; Zhang, L. Evolution of functional properties realized by increasing laser scanning speed for the selective laser melting fabricated NiTi alloy. *J. Alloy. Compd.* **2019**, *804*, 220–229. [CrossRef]
28. Saedi, S.; Moghaddam, N.S.; Amerinatanzi, A.; Elahinia, M.; Karaca, H.E. On the effects of selective laser melting process parameters on microstructure and thermomechanical response of Ni-rich NiTi. *Acta Mater.* **2018**, *144*, 552–560. [CrossRef]
29. Obeidi, M.A.; Monu, M.; Hughes, C.; Bourke, D.; Dogu, M.N.; Francis, J.; Zhang, M.; Ahada, I.U.; Brabazon, D. Laser beam powder bed fusion of nitinol shape memory alloy (SMA). *J. Mater. Res. Technol.* **2021**, *14*, 2554–2570. [CrossRef]
30. Wang, X.; Yu, J.; Liu, J.; Chen, L.; Yang, Q.; Wei, H.; Sun, J.; Wang, Z.; Zhang, Z.; Zhao, G.; et al. Effect of process parameters on the phase transformation behavior and tensile properties of NiTi shape memory alloys fabricated by selective laser melting. *Addit. Manuf.* **2020**, *36*, 101545.
31. Ou, S.-F.; Peng, B.-Y.; Chen, Y.-C.; Tsai, M.-H. Manufacturing and Characterization of NiTi Alloy with Functional Properties by Selective Laser Melting. *Metals* **2018**, *8*, 342. [CrossRef]